

An Artificial Neural Network-Based Model Predictive Control for Three-phase Flying Capacitor Multi-Level Inverter

Parisa Boodaghi Malidarreh*, Abualkasim Bakeer^{†‡¶}, Ihab S. Mohamed^{§¶}, and Lantao Liu[§]

*Dep. of Power Electronics and Elect. Machines, Iran University of Science and Technology (IUST), Iran

[†]Dep. of Elect. Engineering, Faculty of Engineering, Aswan University, Aswan 81542, Egypt

[‡]Dep. of Elect. Power Eng. and Mechatronics, Tallinn University of Technology, 19086 Tallinn, Estonia

[§]Luddy School of Informatics, Computing, and Engineering, Indiana University, Bloomington, IN 47408 USA

Abstract—Model predictive control (MPC) has been used widely in power electronics due to its simple concept, fast dynamic response, and good reference tracking. However, it suffers from parametric uncertainties, since it directly relies on the mathematical model of the system to predict the optimal switching states to be used at the next sampling time. As a result, uncertain parameters lead to an ill-designed MPC. Thus, this paper offers a model-free control strategy on the basis of artificial neural networks (ANNs), for mitigating the effects of parameter mismatching while having a little negative impact on the inverter's performance. This method includes two related stages. First, MPC is used as an expert to control the studied converter in order to provide the training data; while, in the second stage, the obtained dataset is utilized to train the proposed ANN which will be used directly to control the inverter without the requirement for the mathematical model of the system. The case study herein is based on a four-level three-cell flying capacitor inverter. In this study, MATLAB/Simulink is used to simulate the performance of the proposed control strategy, taking into account various operating conditions. Afterward, the simulation results are reported in comparison with the conventional MPC scheme, demonstrating the superior performance of the proposed control strategy in terms of getting low total harmonic distortion (THD) and the robustness against parameters mismatch, especially when changes occur in the system parameters.

Index Terms—Model predictive control, Artificial neural network, Multilevel inverter, Total harmonics distortion.

I. INTRODUCTION

POWER converters have been used in a wide range of applications in recent decades due to their improved performance and efficiency [1]. In this context, substantial attention has been paid to multilevel inverters (MLIs) that introduced with certain advantages, such as: (i) reducing the total harmonic distortion, (ii) reducing common-mode voltage, and (iii) reducing the dv/dt (the rate of voltage change over time in switching instant) stress that leads to a reduction in electromagnetic emissions. There are a number of well-established and conventional MLI topologies that have been implemented

and refined over time, such as: flying capacitor (FC), cascaded H-Bridge (CHB), neutral point clamped (NPC), as well as innovative topologies that combine different topologies to improve MLIs performance [2], [3]. As a result, different control methods have been investigated including various linear methods such as proportional-integral (PI) with pulse width modulation (PWM) or space vector modulation (SVM) [4], [5], non-linear methods with Hysteresis [6], and other non-classical (i.e., modern) control methods such as different techniques of predictive control [6], [7]. However, controlling the MLIs with the high number of switches brings about dire problems in controlling algorithms and makes them more complex. Moreover, voltage imbalance among the MLI capacitors becomes an important concern in designing efficient control algorithms [8]–[11].

Model predictive control, among several control methods described, has appealing aspects that demonstrate its proper functioning. It provides a fast transient response, straightforward implementation, and non-linear constraints consideration [12]–[15]. Furthermore, the development of efficient microprocessors accounts for applying the MPC schemes widely in machine drive, grid-connected converters, and power supplies [16]–[19]. By explicitly utilizing the model of the system to be controlled, MPC selects, at each time step, the optimal switching state that minimizes a pre-defined cost function. However, it has a high *online* computational burden especially when multiple time-horizons are considered, as: (i) the cost function should be calculated for different possible switching states; (ii) the optimization yields the optimal control sequence (i.e., optimal switching states); (iii) the first optimal switching state is finally applied to the system in the next sampling time. Sequentially, it can be quite difficult to employ the MPC to control MLIs with numerous levels [20]–[25]. In addition, as previously mentioned, MPC directly uses the mathematical model of the system, and thus the prediction accuracy is sensitive to the change in system parameters. As a result, it is susceptible to perform incorrectly as a result of parameter variations that may occur in the real system

[¶] Abualkasim Bakeer and Ihab S. Mohamed have contributed equally to this work as a co-second author.

due to degradation and temperature effects [26].

To be more specific, some non-modeled variables, such as temperature and magnetic saturation, have impacts on the real system's parameters that are so-called modeling errors or errors in measurements; these effects can deteriorate the control performance. Therefore, various control techniques have been proposed for tackling and analyzing the effects of parametric uncertainties [27], [28]. On the other hand, since MPC possesses a non-linear structure, these studies were carried out empirically by studying the behavior of MPC under different uncertainty conditions [28], the obtained results led to adjust the model parameters such as inductance to mitigate the effects of the parameter mismatch. Moreover, the negative effects of mismatches in load resistance were ignored [26], [29]. For instance, authors in [29] examined the impact of electrical parameters' variation in six-phase induction motor drive. It has been shown that the parameter of inductance can affect the performance of MPC, especially the stator and rotor leakage. While, in [26], the predictive control-based direct power control with an adaptive parameter identification technique is proposed to cope with the parameter uncertainty problem. In this method, the input resistance and inductance of the converter are estimated using the input current and voltage at each sampling time, without having extra sensors. Thus, the converter parameters are updated online to curb the effects of parameter uncertainty.

Furthermore, the use of data-based control approaches, such as ANN-based control methods, has increased in recent research, particularly in power electronics and motor drives [30]. Just to name a few, in [31], an ANN-based MPC control strategy was introduced to improve the performance of a three-phase inverter with an output LC filter, with comparison to the conventional MPC scheme. While, in [25], a general ANN-MPC scheme is presented to tackle the computational challenge in adopting MPC in highly complex power converters. In [32], the authors proposed a data-based technique for calculating the voltages of capacitors in order to eliminate the need for system sensors. While, an ANN-based method is used in [33] to regulate the weighting factors in the cost function of MPC, which represents one of the research challenges in Model Predictive Control. Moreover, data-based control schemes are used in motor drives for estimating rotor speed, rotor flux, and torque in induction motors [34]–[36].

This paper proposes an artificial neural network-based (ANN-based) control strategy for a three-phase four-level flying capacitor inverter. MPC has been used as a baseline control scheme for (i) collecting the data required for training process, considering different operating conditions, and (ii) assessing our proposed control strategy. The main contributions of the proposed ANN-based control strategy can be summarized as follows:

- 1) It is an *End-to-End* (E2E) control scheme that generates directly the optimal switching states of the inverter, without the need for either the mathemat-

ical model of the inverter and a pre-defined cost function to be minimized at each time step.

- 2) It reduces the effects of the parameter mismatch problems as it offers a model-free control strategy based on ANNs.
- 3) The proposed technique exhibits low THD in the output current compared to the conventional MPC.
- 4) Moreover, the impact of the input features selection on the performance of the proposed control strategy is studied and evaluated.
- 5) Finally, we provide an open repository of the dataset and simulation files to the community for further research activities.

This paper is organized as follows. In Section II, the flying capacitor multilevel inverter (FCMLI) and its mathematical model are briefly described, whereas the model predictive control strategy is explained in Section III. The ANN-based MPC control strategy proposed in this work for the FCMLI is presented in Section IV. In Section V, simulation results for both control strategies are discussed. Finally, conclusions are given in section VI.

II. FLYING CAPACITOR MULTILEVEL INVERTER

Flying capacitor multilevel inverter (FCMLI) comprises a series of connected cells which have a flying capacitor and two switches with antiparallel diodes. These switches are working in a complementary manner to avoid the short-circuit between the flying capacitor terminals. An N -cell FCMLI has $2N$ switches in each leg, and it produces $(N + 1)$ voltage levels from $-\frac{V_{dc}}{2}$ to $\frac{V_{dc}}{2}$, where V_{dc} denotes the input voltage source. The average voltage of each capacitor should be kept fixed at multiples of $\frac{V_{dc}}{N}$. The nearest capacitor to the load has $\frac{V_{dc}}{N}$, whilst the capacitor that is connected to the voltage source has V_{dc} ; the capacitor voltage ratio should be set as $V_{1x} : V_{2x} : V_{3x} = 1 : 2 : 3$ with $x \in \{a, b, c\}$ for generating the four-level voltage waveform. Fig. 1 shows a three-phase four-level flying capacitor (FC) inverter with three cells. Each capacitor's voltage can be estimated using the inverter current i_x and switching states in the corresponding leg, as given in (1) and (2). In addition, for a resistive-inductive load (i.e., RL -load), the three-phase output voltage can be written as in (3), where R and L are the load resistance and inductance, respectively. Table I displays the eight possible switching states of a single-phase FCMLI and the corresponding output voltage.

$$V_{1x} = V_{1x}(0) + \frac{1}{C_{1x}} \int_0^t i_x (S_{2x} - S_{1x}) dt \quad (1)$$

$$V_{2x} = V_{2x}(0) + \frac{1}{C_{2x}} \int_0^t i_x (S_{3x} - S_{2x}) dt \quad (2)$$

$$V_{xN} = Ri_x + L \frac{di_x}{dt} + \frac{1}{3} (V_{aN} + V_{bN} + V_{cN}) \quad (3)$$

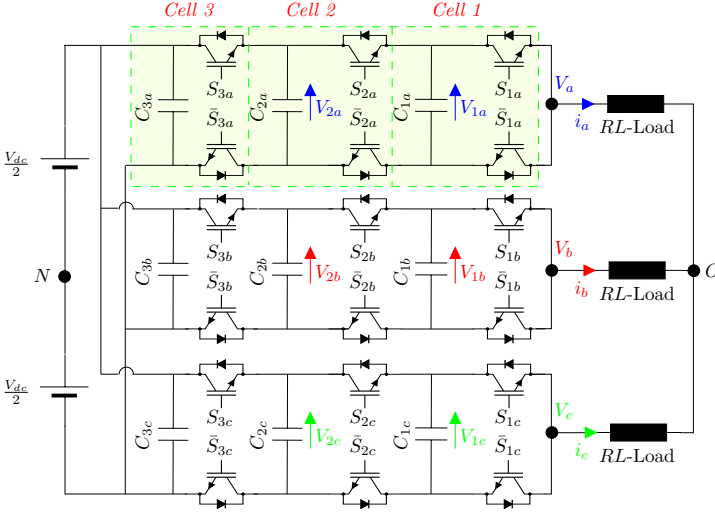


Fig. 1. Topology of a three-phase four-level flying capacitor inverter that is directly connected to an RL -load.

Table I
SWITCHING STATES FOR SINGLE-PHASE FC CONVERTER

V_i	S_{1x}	S_{2x}	S_{3x}	Output voltage V_{xN}	Equation
V_0	0	0	0	$-V_{dc}/2$	$-V_{dc}/2$
V_1	1	0	0	$-V_{dc}/6$	$V_{1x} - V_{dc}/2$
V_2	0	1	0	$-V_{dc}/6$	$V_{2x} - V_{1x} - V_{dc}/2$
V_3	1	1	0	$V_{dc}/6$	$V_{2x} - V_{dc}/2$
V_4	0	0	1	$-V_{dc}/6$	$V_{dc}/2 - V_{2x}$
V_5	1	0	1	$V_{dc}/6$	$V_{dc}/2 - V_{2x} + V_{1x}$
V_6	0	1	1	$V_{dc}/6$	$V_{dc}/2 - V_{1x}$
V_7	1	1	1	$V_{dc}/2$	$V_{dc}/2$

III. MODEL PREDICTIVE CONTROL FOR FCMLI

Model predictive control (MPC) is one of the well-established and promising model-based control methods that is successfully used in power electronics. The key idea behind (MPC) is the use of the system model for predicting the future behavior of the variables to be controlled, considering a certain time horizon. To do so, it needs, in our case, the discrete model of the converter. The optimal control signal, i.e., switching states as described in Table I, that minimizes the cost function is then determined. The entire MPC procedure for FCMLI is shown in Fig. 2, which can be described step-by-step as follows:

- 1) At sampling instant k , the controlled variables (namely, $V_{1x}^k, V_{2x}^k, i_x^k$) should be measured.
- 2) Those controlled variables are then predicted at instant $k+1$ based on the discrete model of the converter given in (4) and (5), where $M_1 = \frac{T_s}{L}$, and $M_2 = 1 - \frac{RT_s}{L}$; while $V_{1x}^{k+1}, V_{2x}^{k+1}, i_x^{k+1}$ are the flying capacitor voltages and output current at instant $k+1$.

$$\begin{aligned} V_{1x}^{k+1} &= V_{1x}^k + \frac{T_s}{C_{1x}} i_x^k (S_{2x}^i - S_{1x}^i) \\ V_{2x}^{k+1} &= V_{2x}^k + \frac{T_s}{C_{2x}} i_x^k (S_{3x}^i - S_{2x}^i) \end{aligned} \quad (4)$$

$$i_x^{k+1} = (V_{xN} - V_{ON})M_1 + i_x^k M_2 \quad (5)$$

where V_{ON} is the common mode voltage.

- 3) After defining a proper cost function J_i , as in (6), it should be calculated for the current switching states S_i based on the desired value of each controlled variable, namely, $V_{1x}^*, V_{2x}^*, i_x^*$.

$$J_i = \lambda_1 (i_x^* - i_x^{k+1})^2 + \lambda_2 (V_{1x}^* - V_{1x}^{k+1})^2 + \lambda_2 (V_{2x}^* - V_{2x}^{k+1})^2 \quad (6)$$

- 4) As the main objective of the optimization problem is to find the optimum switching state (S_{opt}) that minimizes the cost function, the cost function of the current switching state J_i is compared with the smallest previous value e .
- 5) Steps 2) to 4) are repeated for all possible switching states given in Table I.
- 6) Finally, the optimum switching state (S_{opt}) is applied at the next sampling instant.

In Fig. 2, N refers to the total number of the possible switching states, which is equal to 8 in this study.

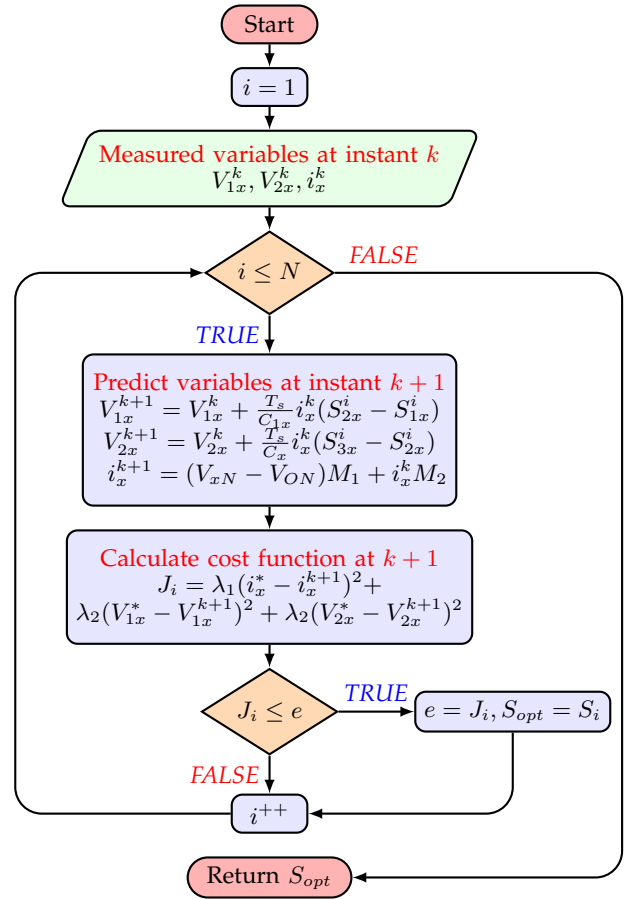


Fig. 2. Flowchart diagram of MPC scheme for FCMLI.

One of the most critical stages of MPC, as previously stated, is determining the switching state (S_{opt}) that minimizes a given cost function. Different forms of cost functions have been established, in this regard, which

are used according to the requirements from the MPC design. In this work, the cost function is expressed as (6), where i_x^* and i_x^{k+1} are the reference and estimated values of the output current at $k + 1$, respectively. Similarly, V_{1x}^{k+1} , V_{2x}^{k+1} and V_{1x}^* , V_{2x}^* refer to the first and second capacitor voltages and their desired values at $k + 1$, respectively. λ_1 and λ_2 are weighting factors of the cost function that determines the importance of the related term in the cost function. For instance, a higher weighting factor indicates the importance of the variable in determining the optimal switching state, thus it shows the priority of that variable in determining the optimal switching state. As previously described, the cost function must be evaluated for all switching states at each sampling time, which can be difficult in systems with many possible switching states such as multilevel inverters; thereby, it needs a strong microprocessor to deal with this high computational burden. In fact, the major drawback of MPC is its optimization procedure that should be solved online, which imposes a large amount of *real-time* calculation. This is an important motivation for proposing an *End-to-End* (E2E) control strategy, such as ANN-Based control strategy, that generates directly the optimal switching states of the inverter, without the need for either: (i) the mathematical model of the inverter and (ii) a pre-defined cost function to be minimized [31].

IV. PROPOSED ANN-BASED CONTROL STRATEGY

A. Overview of ANN

Artificial neural network (ANN) is a subset of machine learning that can be directly defined as a mathematical relationship between input features and targets; in other words, it is a mathematical model that uses learning algorithms to make intelligent decisions based on historical data. It consists of a set of nodes, so-called neurons, that form layers that are connected and executed in parallel.

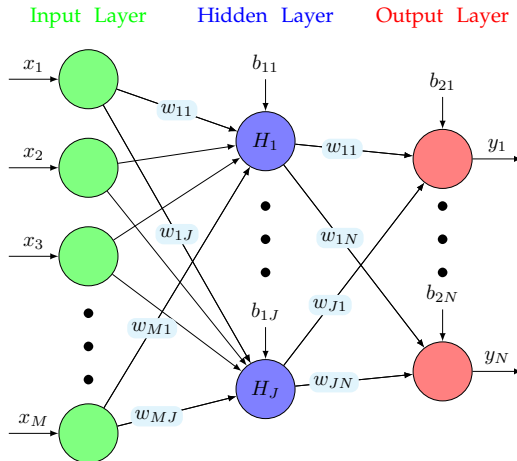


Figure 3. A typical architecture of a two-layer ANN with M inputs, one hidden layer containing J neurons, and N outputs.

Figure 3 shows the typical architecture of a multi-input multi-output ANN that has M input features (i.e., $x_m \forall m = \{1, \dots, M\}$) and yields N output targets (namely, $y_n \forall n = \{1, \dots, N\}$), where the number of neurons in both input and output layers should be equivalent to the number of data to be processed and the number of targets, respectively. Each input feature x_m is multiplied by weighting factors $w_{mj} \forall j = \{1, \dots, J\}$ and applied to the hidden layer. In the hidden layer, the bias b_{1j} is added to the sum of the weighted values and an activation function is applied to it in each neuron; then, the results are multiplied by another weighting factors w_{jn} before being passed to the output layer. Those correction factors (i.e., biases) allow us to shift the activation functions which improves the model's fit to the given dataset. The mathematical formulation of the n^{th} output can be described as:

$$y_n = h \left(\sum_{j=1}^J w_{jn} H_j + b_{2n} \right), \quad \forall n = \{1, \dots, N\}, \quad (7)$$

$$H_j = h \left(\sum_{m=1}^M w_{mj} x_m + b_{1j} \right), \quad \forall j = \{1, \dots, J\},$$

where h is the activation function, H_j are the outputs of the hidden layer, and b_{2n} refer to the biases of the output layer. Activation functions h (such as *sigmoid*, *hyperbolic tangent*, *softmax*, and *linear*) are the key part of the neural network design that are used to learn complicated patterns and assess how well the network model learns the training dataset [37]. Moreover, there exist different learning methods; in this study, the feed-forward method is used. Unlike recurrent neural networks, connections between different nodes in various layers do not produce a cycle in the feed-forward learning approach.

B. ANN-Based Control Strategy

The ANN-based control scheme proposed, in this work, undergoes two main phases, namely, training and testing phases. As mentioned above, the ANN should be first trained *offline*. To do so, MPC has been used as a baseline control scheme for assessing our proposed control strategy and, in the meanwhile, for collecting data required for training, validation, and testing the proposed neural network. The acquired MPC dataset is used to train the ANN to anticipate the optimal switching state S_{opt} at instant $k + 1$. Afterwards, once the proposed neural network is fine-tuned, it can be successfully used *online* for controlling the FCMLI, instead of relying on the predictive control strategies.

In this study, the input features of our proposed ANN-based control scheme are a set of measured variables of the inverter, while the output includes the optimal switching states S_{opt} that should be applied to the inverter at next sampling instant $k + 1$, as illustrated in Fig. 4. More precisely, the output includes a vector of eight elements that identifies the eight voltage vectors

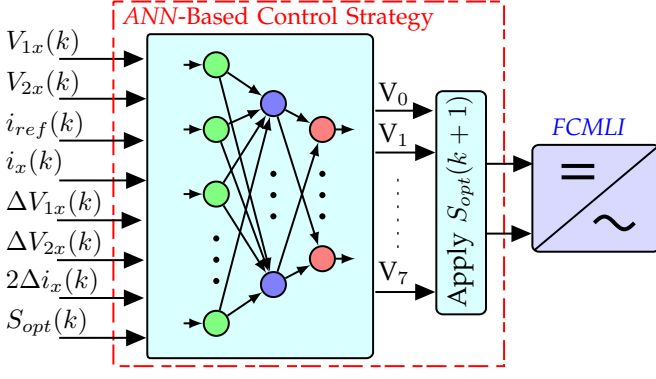


Fig. 4. Block diagram of the ANN-based control strategy, considering $\mathbf{X}_2 = \{V_{1x}, V_{2x}, i_{ref}, i_x, \Delta V_{1x}, \Delta V_{2x}, 2\Delta i_x, S_{opt}\}$ as input features.

($V_i \forall i = \{0, \dots, 7\}$) (see Table I). Each sampling instant, the index of the *optimum* voltage vector will be only active with a value of one, whereas others will be equal to zero.

C. Input Features Selection and Training Process

Basically, selecting the best set of features is a significant part of designing the ANN-based control strategy. Based on the type of inverters and the main purpose of the study, different features can become efficient in both the training phase and testing phase that assess the capability of the learning the mathematical model of the system to be controlled and its dynamics. We have observed that in order to seek the best mapping from the raw input data to the desired outputs, different combinations of input features should be first considered and then assessed. To this end, different operating conditions (i.e., S_1, S_2, \dots, S_{16}) with different system parameters (such as, $V_{dc}, T_s, R, L, i_{ref}$) are considered (see Table II) so that assess five different sets of input features, named: $\mathbf{X}_1, \mathbf{X}_2, \mathbf{X}_3, \mathbf{X}_4$, and \mathbf{X}_5 . As can be seen Table II, for

those input features, the THD of the output current i_x is computed, based on primary samples acquired by MPC, and compared so that the best input features can be chosen. We can observe from the preliminary results that the performance of the proposed control strategy on the basis of \mathbf{X}_5 , in which the lowest set of features is used, is the worst as the THD is quite higher. Furthermore, it can be observed that the four-level output voltage V_{ph} that has been added to \mathbf{X}_1 does not have much improvement. For that reason, \mathbf{X}_2 is selected as input features for the proposed control scheme that given in Fig. 4, due to its significant improvement compared to other considered sets. \mathbf{X}_2 is composed of 8 measurable variables, namely: $\{V_{1x}, V_{2x}, i_{ref}, i_x, \Delta V_{1x}, \Delta V_{2x}, 2\Delta i_x, S_{opt}\}$, where $\Delta V_{1x} = (\frac{V_{dc}}{3} - V_{1x})$, $\Delta V_{2x} = (\frac{2V_{dc}}{3} - V_{2x})$, $\Delta i_x = (i_{ref} - i_x)$, and S_{opt} is the optimal switching state at time instant k .

Once the effective set of features is selected, MPC is utilized for providing the required dataset. The dataset is collected taken into account different uncertainties in the converter parameters such as input voltage, cell capacitance, RL impedance, reference load current, and sampling period, as listed in Table III. Only eleven different conditions are applied to the FC inverter, where the nominal values of the converter parameters are as follows: $V_{dc} = 360$ V, $C = 680$ μ F, $L = 10$ mH, $R = 15$ Ω , $i_{ref} = 15$ A, The MPC's sampling time is indicated in the last column. In this work, the total dataset is randomly divided into three sets: training set, validation set, and testing set with 70%, 15%, and 15% of the total dataset, respectively. The optimum number of hidden layers is determined by varying the number of hidden layers and observe the testing accuracy. In addition, the *transcg* function is used as a training function. After the training process, the trained ANN can be used to control the four-level three-phase flying capacitor inverter. The training confusion matrix that assesses the performance of the training is shown in Fig. 5, where the lowest validation error is 0.1016 taken from epoch 701 and the overall accuracy is 89.80% with the total instances numbers of

Table II

THD OF THE OUTPUT CURRENT i_x FOR DIFFERENT SETS OF INPUT FEATURES, WHERE THE LOWEST THD IS HIGHLIGHTED IN BLUE.

Sample No.	S_1	S_2	S_3	S_4	S_5	S_6	S_7	S_8	S_9	S_{10}	S_{11}	S_{12}	S_{13}	S_{14}	S_{15}	S_{16}
V_{dc} [V]	360	360	360	342	378	360	360	350	340	360	360	340	350	360	350	350
T_s [μ s]	30	30	30	20	20	20	45	50	50	50	20	25	20	20	25	40
R [Ω]	10	15	25	7.5	15	15	8	9	11	10	10	10	12	7	9	9
L [mH]	5	10	12	8	4.5	9	10	9.5	5	5.5	5	5	7	5	5	5
i_{ref} [A]	17	12	5	12	10	4	5	6	6	4.35	12	10	8	15	12	12
$\mathbf{X}_1 = \{V_{c1}, V_{c2}, i_{ref}, i_x, \Delta V_{c1}, \Delta V_{c2}, \Delta i_x, S_{opt}, V_{ph}\}$																
THD [%]	1.89	1.29	3.09	1.30	2.02	4.54	3.51	3.22	6.48	8.88	1.44	2.01	1.85	1.40	1.73	2.68
$\mathbf{X}_2 = \{V_{c1}, V_{c2}, i_{ref}, i_x, \Delta V_{c1}, \Delta V_{c2}, 2\Delta i_x, S_{opt}\}$																
THD [%]	1.65	1.06	2.36	0.93	2.07	4.13	3.73	3.17	6.22	8.01	1.41	2.21	1.25	1.20	1.69	3.06
$\mathbf{X}_3 = \{V_{c1}, V_{c2}, i_{ref}, i_x, \Delta V_{c1}, \Delta V_{c2}, \Delta i_x, S_{opt}\}$																
THD [%]	1.90	1.32	3.28	1.36	1.94	4.38	3.78	3.37	6.29	8.11	1.47	1.98	1.43	1.22	1.74	2.69
$\mathbf{X}_4 = \{V_{c2}, i_{ref}, i_x, \Delta V_{c1}, \Delta V_{c2}, \Delta i_x, S_{opt}\}$																
THD [%]	1.59	1.31	3.64	1.08	2.08	4.39	3.53	3.22	6.57	7.98	1.43	2.03	1.71	1.74	1.69	2.67
$\mathbf{X}_5 = \{i_{ref}, i_x, \Delta V_{c1}, \Delta V_{c2}, \Delta i_x, S_{opt}\}$																
THD [%]	2.69	1.45	3.53	1.32	2.04	4.55	3.71	3.50	6.62	8.11	1.81	2.11	1.65	1.76	1.99	2.94

509,788. The training results are summarized in Table IV, demonstrating that the training dataset based on \mathbf{X}_2 is properly selected, resulting in an efficient control system.

Table III
TRAINING CONDITIONS OF ANN-BASED CONTROL STRATEGY.

Condition No.	$V_{dc} = 360$ [V]	$C = 680$ [μ F]	$L = 10$ [mH]	$R = 15$ [Ω]	$i_{ref} = 15$ [A]	T_s [μ s]
C_1	0.95	0.95	1.00	0.80	0.95	30
C_2	0.90	0.85	0.95	0.70	0.90	10
S_3	1.25	0.90	1.20	1.10	1.15	50
C_4	1.10	1.05	1.50	1.23	1.05	60
C_5	1.00	1.10	1.05	1.40	0.75	15
C_6	1.00	0.98	0.75	1.30	0.65	18
C_7	1.15	1.20	0.80	1.17	0.55	50
C_8	1.00	1.07	0.88	0.77	0.85	30
C_9	1.00	1.00	0.98	0.87	0.50	40
C_{10}	1.00	1.00	0.90	0.10	2.00	5
C_{11}	1.00	1.00	0.90	0.10	2.00	15

1	21347 13.6%	0 0.0%	235 0.1%	340 0.2%	254 0.2%	0 0.0%	0 0.0%	0 0.0%	96.3% 3.7%
2	0 0.0%	21459 13.6%	0 0.0%	0 0.0%	0 0.0%	300 0.2%	284 0.2%	298 0.2%	96.1% 3.9%
3	358 0.2%	0 0.0%	16889 10.7%	732 0.5%	890 0.6%	324 0.2%	137 0.1%	30 0.0%	87.2% 12.8%
4	258 0.2%	0 0.0%	963 0.6%	15247 9.7%	760 0.5%	141 0.1%	8 0.0%	85 0.1%	87.3% 12.7%
5	297 0.2%	0 0.0%	951 0.6%	856 0.5%	17172 10.9%	8 0.0%	130 0.1%	253 0.2%	87.3% 12.7%
6	0 0.0%	272 0.2%	206 0.1%	121 0.1%	5 0.0%	16963 10.8%	680 0.4%	940 0.6%	88.4% 11.6%
7	0 0.0%	254 0.2%	169 0.1%	0 0.0%	125 0.1%	911 0.6%	15415 9.8%	843 0.5%	87.0% 13.0%
8	0 0.0%	285 0.2%	14 0.0%	151 0.1%	359 0.2%	912 0.6%	888 0.6%	16981 10.8%	86.7% 13.3%
	95.9% 4.1%	96.4% 3.6%	86.9% 13.1%	87.4% 12.6%	87.8% 12.2%	86.7% 13.3%	87.9% 12.1%	87.4% 12.6%	89.8% 10.2%
	1	2	3	4	5	6	7	8	
	Target Class								

Fig. 5. Training confusion matrix for 70% training set with a misclassification error of 10.2%, where the number of correctly and incorrectly classified observations are shown in green and red, respectively.

Table IV
TRAINING RESULTS.

No. instances	Accuracy	Error (Epoch)
509,788	89.80%	0.1016(701)

V. SIMULATION RESULTS AND DISCUSSION

In this section, the ANN-based control strategy is simulated using MATLAB/Simulink software and its performance is compared to that of the conventional MPC. The parameters of the FCMLI given in Fig. 1 are listed in Table V.

Table V
PARAMETERS OF THE FCMLI.

Parameter	Value
R	15 [Ω]
L	10 [mH]
C	680 [μ F]
V_{dc}	360 [V]
T_s	30 [μ s]
f	50 [Hz]

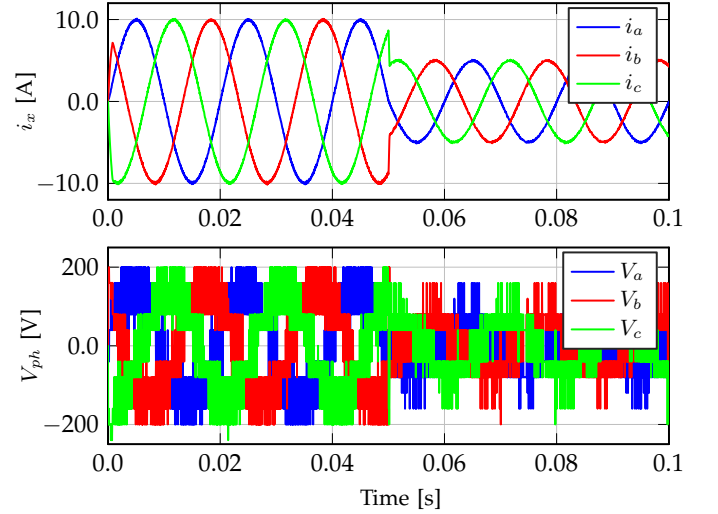


Fig. 6. Dynamic response of ANN-based control strategy: Output current and voltage when the reference current i_{ref} changes from $i_{ref} = 10$ A to $i_{ref} = 5$ A at $t = 0.05$ s.

The dynamic behavior of the ANN-based and MPC control schemes are illustrated in Figs. 6 and 7, respectively. Both figures show the load output current i_x and four-level output voltage V_{ph} under a sudden change of reference current i_{ref} from 10 A to 5 A at $t = 0.05$ s. It is observed that both methods have similar and good performance under dynamic conditions, since both control strategies track the reference current properly.

The behavior of our proposed ANN-based control strategy under steady-state condition is depicted in Fig. 8, while the behavior of the classical MPC is shown in

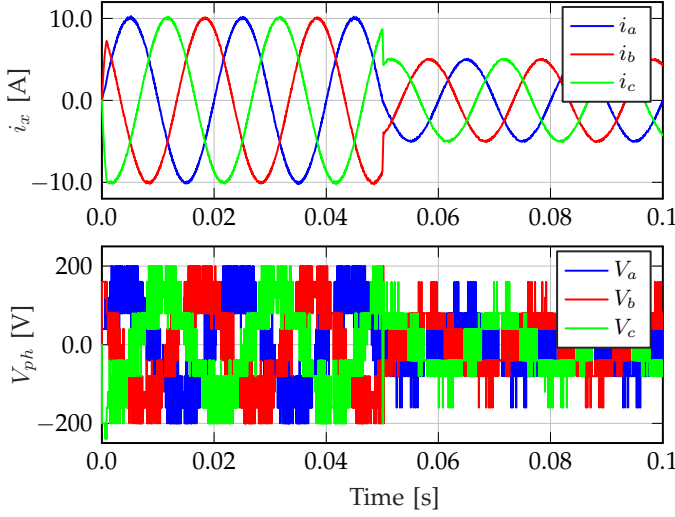


Fig. 7. Dynamic response of MPC: output current and voltage when the reference current i_{ref} changes from $i_{ref} = 10$ A to $i_{ref} = 5$ A at $t = 0.05$ s.

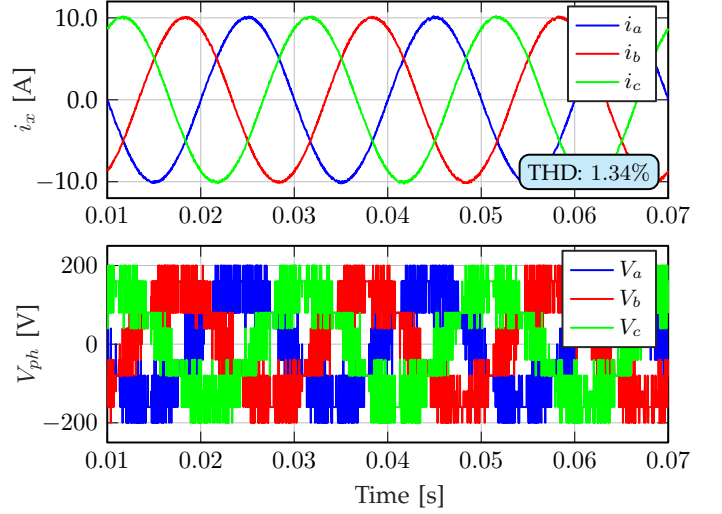


Fig. 9. Simulation results of MPC: Output current and four-level voltage

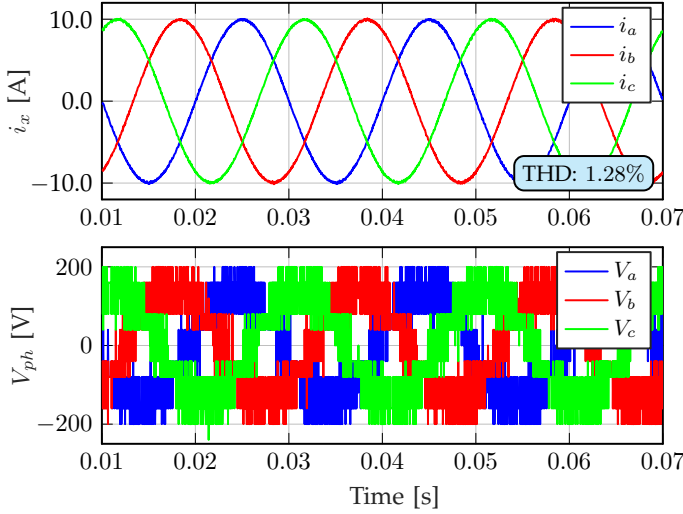


Fig. 8. Simulation results of ANN-based control strategy: Output current and four-level voltage.

Fig. 9. It can be seen in the figures that the two control strategies generate a high-quality sinusoidal output current i_x with low distortion. However, the THD of the output current in the case of an ANN-based control scheme is slightly lower than that in the case of MPC, namely, 1.34% compared to 1.28% in case of ANN-based method. For more information, the frequency spectrum of the two control methods are shown in Figs. 10 and 11. In addition, the voltages of the capacitors (i.e., V_{1x} , V_{2x}) obtained by the two proposed control strategies are depicted in Figs. 12 and 13, respectively. As can be observed, our proposed control scheme has a proper performance to keep the voltage at its desired value as well as the MPC scheme.

As previously described, the ANN-based control strategy can be used to deal with the parameter uncertainty

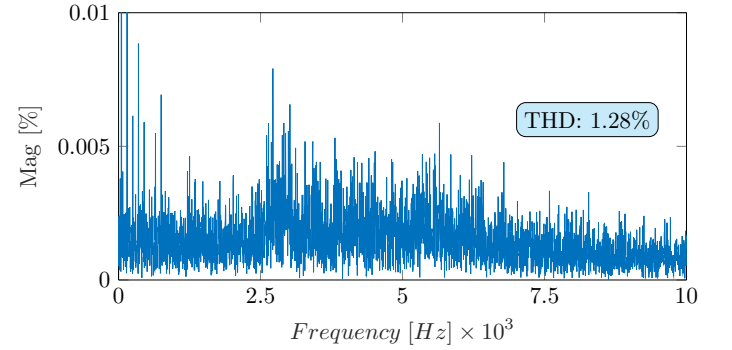


Fig. 10. Frequency spectrum of output current for the ANN-based control strategy.

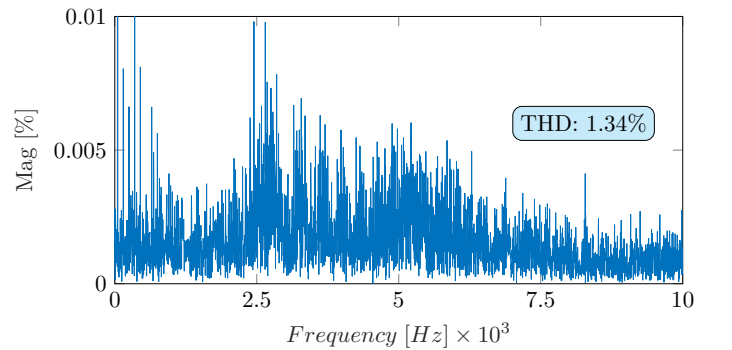


Fig. 11. Frequency spectrum of output current for the MPC.

issues that arise in real systems. Thus, to verify the efficiency of the ANN-based MPC technique in this scope, another simulation study is carried out, where both control strategies are utilized to compare their performance under this condition. More precisely, the load inductance L is changed from 10 mH to 5 mH at

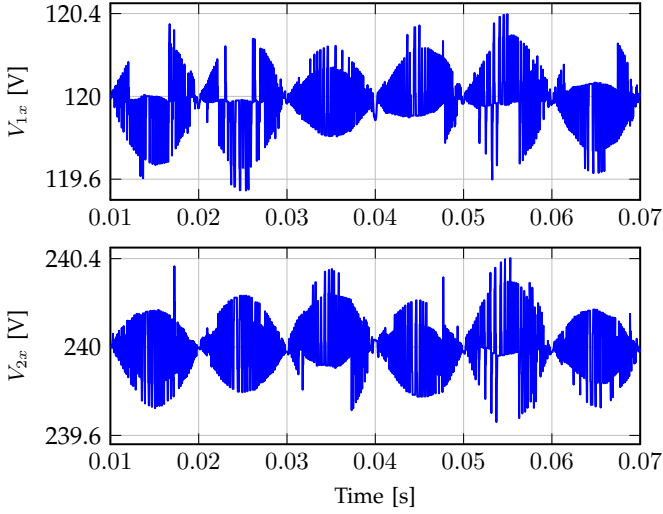


Fig. 12. Simulation results of ANN-based control strategy: Voltages of the capacitors.

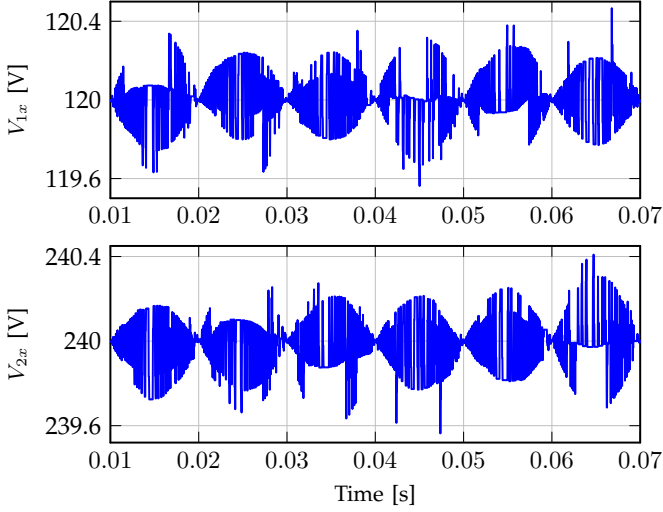


Fig. 13. Simulation results of MPC: Voltages of the capacitors.

$t = 0.1$ s; the obtained results are depicted in Figs. 14 and 15. By comparison between these two figures, it can be seen that the proposed ANN-based control scheme has better performance in such a situation. This can be clearly seen in the *THD* of the output current for the ANN-based control scheme that has a 2.78% compared to 3.05% in the case of MPC after changing the inductance value, which demonstrates that the proposed control scheme is more robust to the parameter uncertainty than the classical MPC.

To better assess and show the superiority of the proposed control strategy in learning the mathematical model of the inverter and its dynamics, a comparison of the *THD* of the output current obtained by the two control strategies is represented in Fig. 16, considering the different operating conditions listed in Table II. The obtained results demonstrate that the proposed ANN-

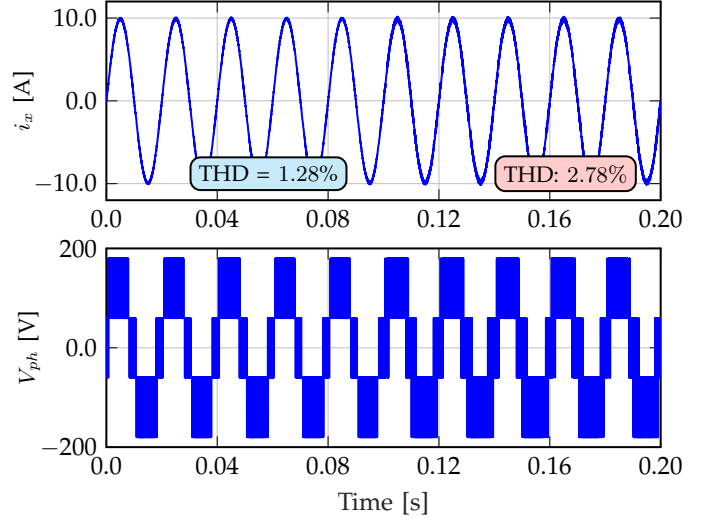


Fig. 14. Performance of our proposed ANN-based control strategy under load inductance variation from $L = 10$ mH to $L = 5$ mH at $t = 0.1$ s.

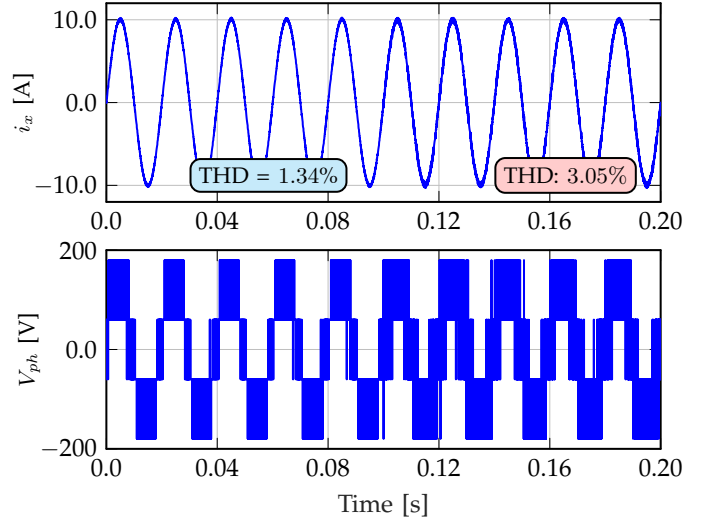


Fig. 15. Performance of the MPC scheme under load inductance variation from $L = 10$ mH to $L = 5$ mH at $t = 0.1$ s.

based control scheme on the basis of the selected input feature (namely, X_2) has good performance compared to the conventional MPC, without requiring a large amount of training data.

VI. CONCLUSIONS AND FUTURE WORK

In this paper, we have proposed an ANN-based control strategy for controlling a three-phase four-level flying capacitor inverter with the aim of generating a high-quality sinusoidal output current and improving the robustness against parametric mismatches, especially when compared to conventional MPC scheme. The proposed control scheme employs the classical MPC to generate a reliable dataset of inverter variables to be used as input features by the proposed a feed-forward ANN. Afterwards, once the *off-line* training is performed

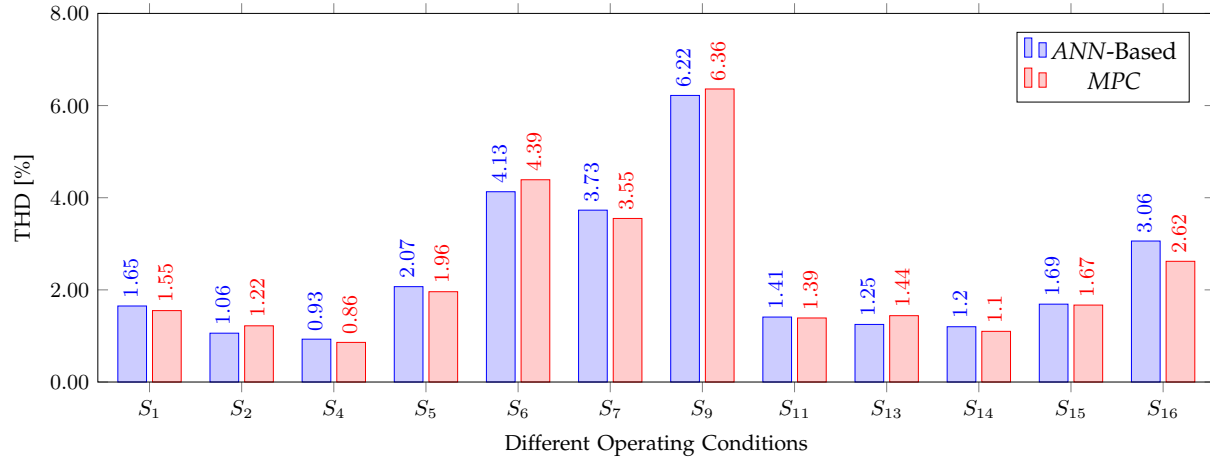


Fig. 16. THD comparison of output current between MPC and ANN-based control strategy.

based on the obtained data from MPC, it can be used to directly control the inverter without the requirement for a mathematical model of the system. Simulation results reveal that ANN-based control strategy performs better with respect to the THD under most conditions. Additionally, an experiment is carried out for assessing its robustness against parameter uncertainty. According to the results, the proposed control scheme showed better performance than the conventional MPC under parameter mismatch conditions, owing to the fact that, unlike MPC, the proposed technique does not depend on the system model. One of the possible directions for future work would be the implementation of the ANN-based control strategy in practical applications.

REFERENCES

- [1] P. Cortés, G. Ortiz, J. I. Yuz, J. Rodríguez, S. Vazquez, and L. G. Franquelo, "Model predictive control of an inverter with output LC filter for UPS applications," *IEEE Transactions on industrial electronics*, vol. 56, no. 6, pp. 1875–1883, 2009.
- [2] P. B. Malidarreh, D. A. Khaburi, and J. Rodríguez, "Capacitor voltage imbalance reduction in flying capacitor modular multilevel converters by using model predictive control," in *2020 11th Power Electronics, Drive Systems, and Technologies Conference (PEDSTC)*. IEEE, 2020, pp. 1–4.
- [3] T. G. Habetler, R. Naik, and T. A. Nondahl, "Design and implementation of an inverter output LC filter used for dv/dt reduction," *IEEE Transactions on Power Electronics*, vol. 17, no. 3, pp. 327–331, 2002.
- [4] J. Jung, M. Dai, and A. Keyhani, "Optimal control of three-phase pwm inverter for ups systems," in *2004 IEEE 35th Annual Power Electronics Specialists Conference (IEEE Cat. No. 04CH37551)*, vol. 3. IEEE, 2004, pp. 2054–2059.
- [5] I. S. Mohamed, S. A. Zaid, M. Abu-Elyazeed, and H. M. Elsayed, "Model predictive control—a simple and powerful method to control UPS inverter applications with output LC filter," in *2013 Saudi International Electronics, Communications and Photonics Conference*. IEEE, 2013, pp. 1–6.
- [6] —, "Classical methods and model predictive control of three-phase inverter with output LC filter for UPS applications," in *2013 International Conference on Control, Decision and Information Technologies (CoDIT)*. IEEE, 2013, pp. 483–488.
- [7] J. Rodríguez and P. Cortes, *Predictive control of power converters and electrical drives*, 1st ed. John Wiley & Sons, 2012.
- [8] S. Kouro, M. Malinowski, K. Gopakumar, J. Pou, L. G. Franquelo, B. Wu, J. Rodríguez, M. A. Pérez, and J. I. Leon, "Recent advances and industrial applications of multilevel converters," *IEEE Transactions on industrial electronics*, vol. 57, no. 8, pp. 2553–2580, 2010.
- [9] S. Kouro, J. Rodríguez, B. Wu, S. Bernet, and M. Perez, "Power the future of industry," *IEEE Trans. Ind. Electron.*, pp. 26–38, 2012.
- [10] J. Rodríguez, S. Bernet, B. Wu, J. O. Pontt, and S. Kouro, "Multi-level voltage-source-converter topologies for industrial medium-voltage drives," *IEEE Transactions on industrial electronics*, vol. 54, no. 6, pp. 2930–2945, 2007.
- [11] L. G. Franquelo, J. Rodríguez, J. I. Leon, S. Kouro, R. Portillo, and M. A. Prats, "The age of multilevel converters arrives," *IEEE industrial electronics magazine*, vol. 2, no. 2, pp. 28–39, 2008.
- [12] J. Rodríguez, M. P. Kazmierkowski, J. R. Espinoza, P. Zanchetta, H. Abu-Rub, H. A. Young, and C. A. Rojas, "State of the art of finite control set model predictive control in power electronics," *IEEE Transactions on Industrial Informatics*, vol. 9, no. 2, pp. 1003–1016, 2012.
- [13] P. Cortés and J. Rodríguez, "Three-phase inverter with output LC filter using predictive control for UPS applications," in *2007 European Conference on Power Electronics and Applications*. IEEE, 2007, pp. 1–7.
- [14] S. Kwak and J.-C. Park, "Switching strategy based on model predictive control of VSI to obtain high efficiency and balanced loss distribution," *IEEE Transactions on Power Electronics*, vol. 29, no. 9, pp. 4551–4567, 2013.
- [15] I. S. Mohamed, S. A. Zaid, M. Abu-Elyazeed, and H. M. Elsayed, "Improved model predictive control for three-phase inverter with output LC filter," *International Journal of Modelling, Identification and Control*, vol. 23, no. 4, pp. 371–379, 2015.
- [16] F. Defaÿ, A.-M. Llor, and M. Fadel, "Direct control strategy for a four-level three-phase flying-capacitor inverter," *IEEE Transactions on Industrial Electronics*, vol. 57, no. 7, pp. 2240–2248, 2010.
- [17] G. Papafotiou, J. Kley, K. G. Papadopoulos, P. Bohren, and M. Morari, "Model predictive direct torque control—part II: Implementation and experimental evaluation," *IEEE Transactions on industrial electronics*, vol. 56, no. 6, pp. 1906–1915, 2008.
- [18] Z. Song, W. Chen, and C. Xia, "Predictive direct power control for three-phase grid-connected converters without sector information and voltage vector selection," *IEEE Transactions on Power Electronics*, vol. 29, no. 10, pp. 5518–5531, 2013.
- [19] I. S. Mohamed, S. A. Zaid, M. Abu-Elyazeed, and H. M. Elsayed, "Implementation of model predictive control for three-phase inverter with output LC filter on eZdsp F28335 Kit using HIL simulation," *International Journal of Modelling, Identification and Control*, vol. 25, no. 4, pp. 301–312, 2016.
- [20] R. Findeisen, F. Allgöwer, and L. T. Biegler, "Assessment and future directions of nonlinear model predictive control," in *Lecture Notes in Control and Information Sciences*, M. Thoma and M. Morari, Eds. Springer, 2007, vol. 358, no. 7.
- [21] M. Nauman and A. Hasan, "Efficient implicit model-predictive control of a three-phase inverter with an output LC filter," *IEEE Transactions on Power Electronics*, vol. 31, no. 9, pp. 6075–6078, 2016.
- [22] C. Garcia, M. Mohammadinodoushan, V. Yaramasu, M. Norambuena, A. Davari, Z. Zhang, D. Khaburi, and J. Rodríguez, "FCS-MPC based pre-filtering stage for computational efficiency in a flying capacitor converter," *IEEE Access*, 2021.

- [23] M. Norambuena, C. Garcia, J. Rodriguez, and P. Lezana, "Finite control set model predictive control reduced computational cost applied to a flying capacitor converter," in *IECON 2017-43rd Annual Conference of the IEEE Industrial Electronics Society*. IEEE, 2017, pp. 4903–4907.
- [24] C. Garcia, M. Norambuena, J. Rodriguez, M. Khosravi, and D. A. Khaburi, "Finite set model predictive control of a flying capacitor converter with a geometric computational optimization," in *2017 IEEE Southern Power Electronics Conference (SPEC)*. IEEE, 2017, pp. 1–5.
- [25] D. Wang, Z. J. Shen, X. Yin, S. Tang, X. Liu, C. Zhang, J. Wang, J. Rodriguez, and M. Norambuena, "Model predictive control using artificial neural network for power converters," *IEEE Transactions on Industrial Electronics*, 2021.
- [26] S. Kwak, U.-C. Moon, and J.-C. Park, "Predictive-control-based direct power control with an adaptive parameter identification technique for improved AFE performance," *IEEE Transactions on Power Electronics*, vol. 29, no. 11, pp. 6178–6187, 2014.
- [27] C. Martin, M. Bermúdez, F. Barrero, M. R. Arahál, X. Kestelyn, and M. J. Durán, "Sensitivity of predictive controllers to parameter variation in five-phase induction motor drives," *Control Engineering Practice*, vol. 68, pp. 23–31, 2017.
- [28] H. A. Young, M. A. Perez, and J. Rodriguez, "Analysis of finite-control-set model predictive current control with model parameter mismatch in a three-phase inverter," *IEEE Transactions on Industrial Electronics*, vol. 63, no. 5, pp. 3100–3107, 2016.
- [29] B. Bogado, F. Barrero, M. R. Arahál, S. Toral, and E. Levi, "Sensitivity to electrical parameter variations of predictive current control in multiphase drives," in *IECON 2013 39th Annual Conference of the IEEE Industrial Electronics Society*. IEEE, 2013, pp. 5215–5220.
- [30] B. Karanayil and M. F. Rahman, "Artificial neural network applications in power electronics and electrical drives," in *Power Electronics Handbook*. Elsevier, 2011, pp. 1139–1154.
- [31] I. S. Mohamed, S. Rovetta, T. D. Do, T. Dragicević, and A. A. Z. Diab, "A neural-network-based model predictive control of three-phase inverter with an output *LC* filter," *IEEE Access*, vol. 7, pp. 124737–124749, 2019.
- [32] X. Liu, L. Qiu, Y. Fang, Z. Peng, and D. Wang, "Finite-level-state model predictive control for sensorless three-phase four-arm modular multilevel converter," *IEEE Transactions on Power Electronics*, vol. 35, no. 5, pp. 4462–4466, 2019.
- [33] T. Dragičević and M. Novak, "Weighting factor design in model predictive control of power electronic converters: An artificial neural network approach," *IEEE Transactions on Industrial Electronics*, vol. 66, no. 11, pp. 8870–8880, 2018.
- [34] M. T. Wishart and R. G. Harley, "Identification and control of induction machines using artificial neural networks," *IEEE Transactions on Industry Applications*, vol. 31, no. 3, pp. 612–619, 1995.
- [35] H.-Y. Lee, J.-I. Lee, S.-O. Kwon, and S.-W. Lee, "Performance estimation of induction motor using artificial neural network," in *2018 25th International Conference on Systems, Signals and Image Processing (IWSSIP)*. IEEE, 2018, pp. 1–3.
- [36] X. Sun, L. Chen, Z. Yang, and H. Zhu, "Speed-sensorless vector control of a bearingless induction motor with artificial neural network inverse speed observer," *IEEE/ASME Transactions on mechatronics*, vol. 18, no. 4, pp. 1357–1366, 2012.
- [37] K. Hornik, "Approximation capabilities of multilayer feedforward networks," *Neural networks*, vol. 4, no. 2, pp. 251–257, 1991.